

Interplanetary scintillation observations of 57 flat-spectrum sources at 327 MHz

Usha Vijayanarasimha, S. Ananthakrishnan and

G. Swarup *Radio Astronomy Centre, Tata Institute of Fundamental Research
PO Box 8, Ootacamud 643 001, India*

Accepted 1984 August 31. Received 1984 July 30

Summary. From interplanetary scintillation observations of an unbiased sample of 57 flat-spectrum radio sources at 327 MHz, we have determined compactness parameters, μ , giving the fraction of the total flux density arising from the compact cores. It is found that the median value of $\mu=0.61$ and the size of the compact cores is ≤ 0.05 arcsec for about half the cases. From VLA data at 5 GHz, the cores are found to have inverted spectra with $\alpha(5000, 327) = -0.16$ on average. Typically the fraction of the total flux density arising from the extended components ≤ 0.04 at 5 GHz, ~ 0.1 at 1 GHz and 0.39 at 327 MHz.

The observed $N(\mu)$ distribution at 327 MHz is consistent with the predictions of the Orr & Browne model, in which only the core of a classical double radio source gets Doppler boosted. However, the observed asymmetry in the structures of many flat-spectrum sources indicates that either the asymmetry is intrinsic, or a three-component model, having a relativistic core, a mildly relativistic kiloparsec-scale jet or hotspot and non-relativistic diffuse radio lobes, is required to explain flat-spectrum sources.

1 Introduction

Recent observations of flat-spectrum radio sources, which are mostly quasars, have revealed the existence of weak extended features of size several arcsec lying close to the bright compact cores of size ≤ 0.1 arcsec. The fraction of the flux density in the extended features is only a few per cent at 5 GHz (Perley 1982) but increases to about 10 per cent at 1 GHz (Moore *et al.* 1981). A 'unified' scheme has been recently suggested by Orr & Browne (1982, hereafter referred to as OB82) in which the flat-spectrum sources are considered to be normal double radio sources, with the source axes pointed close to the line-of-sight so that the emission from their weak nuclear components gets Doppler boosted as a result of bulk relativistic motion. In this scheme, the extended features are identified with the outer radio lobes of steep spectrum. However, it has also been shown that the radio structures of many of the well-resolved flat-spectrum sources are much more asymmetric than those for the normal double sources (Perley, Fomalont & Johnston 1980; Browne *et al.* 1982; Perley 1982). Although statistics are not available for complete samples, brightness ratios for the two lobes of $\geq 4:1$ have been observed in many cases. Since the extended

features have steep spectra, a study at metre wavelengths is likely to be valuable for understanding their nature.

In this paper, we describe interplanetary scintillation (IPS) observations of an unbiased sample of 57 flat-spectrum radio sources at 327 MHz using the Ooty Radio Telescope (Swarup *et al.* 1971). The observations were carried out during 1981–82 and allowed detection of compact scintillating components of flux density $S_{\text{obs}} \geq 50$ mJy and angular size between <50 to 500 milliarcsec. The results obtained are compared with the predictions of the OB82 model.

2 Observations and analysis

A sample of 91 radio sources was selected from the compilation made by Kuhr *et al.* (1981), after satisfying the following criteria:

$$S_{5000} \geq 1 \text{ Jy}, \alpha_{400}^{5000} \leq 0.5 (S_v \propto v^{-\alpha}), -35^\circ < \delta < +35^\circ$$

but including only those sources which lie at $|b| \geq 10^\circ$ as well as within 20° of the Sun's path. Values of S_{408} given by Large *et al.* (1981) were also considered. IPS observations could be carried out only for 57 sources during 1981–82. This is, nevertheless, an unbiased sample because no *a priori* information, such as flux density or radio structure or spectrum, was used in limiting the observations to these 57 sources.

The method of IPS data reduction is briefly described below. Further details can be found in Rao, Bhandari & Ananthkrishnan (1974). A bandwidth of 4 MHz and a time constant of 50 ms were used. Each source was tracked for about 20–30 min and the output recorded digitally with a sampling rate of 50 samples s^{-1} . Although the level of radio interference at Ootacamund is low, any interference spikes are easily identified and removed because the Ooty Radio Telescope provides 12 simultaneous adjacent beams. Mean and variance of the data are calculated and the power spectrum for each minute is computed using a 2048-point FFT algorithm with a final resolution of 0.1 Hz. After adding the spectra for individual 1-min data stretches, the resultant spectrum is corrected for the time-constant attenuation function. The 'OFF-source' data are also processed similarly. The two parameters estimated from the 'ON' spectra are (1) the second moment, f_2 , which indicates the width of the power spectrum and (2) the rms of the intensity fluctuations, S_{obs} , which is the square root of the area under the power spectrum. The gain of the radio telescope is determined by observing one of the standard flux calibrators used at Ooty at 327 MHz.

Each source was observed in this manner at several solar elongations $\epsilon > 8^\circ$, the value below which strong scattering starts to quench the scintillations appreciably. The angular size ψ of the scintillating component was estimated by comparing the ratios of the observed f_2 values at each ϵ with the corresponding values measured by us for the compact IPS calibrator, namely the radio source 1148–001, and then taking a weighted average. From extensive IPS and VLBI observations of 1148–001, its angular size is estimated to be in the range 30–50 milliarcsec at 327 MHz (Brotten *et al.* 1969; Galt *et al.* 1977; Venugopal *et al.*, in preparation). We have therefore taken all the flat-spectrum sources whose second moments are less than those of 1148–001, at the corresponding values of ϵ , to be resolved and estimated their angular size ψ using the above-mentioned ratio (Rao *et al.* 1974). Sources whose second moments are comparable to that of 1148–001 are considered unresolved with $\psi \leq 50$ milliarcsec. Further, since diameter blurring attenuates scintillations for components with large angular size, the IPS technique at 327 MHz is sensitive only to sources with sizes $\psi \leq 0.5$ arcsec.

The compactness parameter defined as $\mu = (S_c/S_{327})$, where S_c and S_{327} are the estimated flux densities of the scintillating components and of the entire radio source respectively, was determined as follows. A weighted average was taken of the measured daily values

$S_c = (FS_{\text{obs}}/m_0)$ where m_0 is the expected rms of intensity fluctuations for a point source of 1 Jy based on the data of the compact radio source 1148-001 at the same elongation ϵ , and F is a correction factor dependent on the value of ψ (Rao *et al.* 1974). Similarly an average was taken of the observed values S_{327} . For many of the observed sources, $S_{327} < 1.5$ Jy which is below the confusion level of the Ooty Radio Telescope. Therefore, for the sake of uniformity S_{327} was estimated for each source from its spectrum (Kuhr *et al.* 1981; Large *et al.* 1982; our measurements for $S_{327} > 1.5$ Jy were also considered). The flux density is on the scale of Baars *et al.* (1977). Since the confusion limit for the flux density of the scintillating components ≤ 0.1 Jy at 327 MHz, values of S_c are determined to within about 20 per cent, the errors arising mainly due to solar wind fluctuations from day to day.

Table 1. Results of the IPS observations at 327 MHz.

Source	Other names	Opt. id.	S_c (327)	No. obs.	S_{327}	μ	ψ	S_c (5000)	5000 σ_{327} (score)	Str.
(1)	(2)	(3)	Jy (4)	(5)	Jy (6)	(7)	arcsec (8)	Jy (9)	(10)	(11)
0003-066		G	1.5±0.3	4	2.0±0.15	0.75	≤ 0.05	1.25	+0.70	A
0048-097	OB081	BL	0.5±0.15	7	1.0±0.2	0.50	0.15	1.12	-0.30	A
0056-001	4C-00.06	Q	3.2±0.4	21	4.0±0.2	0.80	≤ 0.05	1.37	+0.31	U
0106+013	4C+01.02	Q	1.4±0.4	7	3.0±0.2	0.47	≤ 0.05	4.55	-0.43	A
0112-017		Q	1.7±0.5	4	1.2±0.1	1.0	≤ 0.05	1.16	+0.14	A
0116+31	4C+31.04	G	2.6	1	3.5±0.2	0.74	≤ 0.05	1.48	+0.21	U
0119+041		Q	0.6±0.2	3	1.0±0.15	0.60	≤ 0.05	0.85	-0.13	T
0122-003		Q	0.7±0.1	3	1.8±0.2	0.39	≤ 0.05	1.29	-0.22	R?
0146+056		Q	0.8±0.1	3	1.0±0.1	0.80	≤ 0.05	1.09	-0.11	U
0202+14	4C+15.05	Q	4.0±0.6	3	5.3±0.5	0.75	0.25	3.62	+0.04	U
0221+067	4C+06.11	Q	0.4	1	1.5±0.2	0.27	0.1	0.74	-0.23	RA
0234+285	4C+28.07	Q	0.7±0.15	4	1.8±0.2	0.39	0.1	2.36	-0.45	?
0235+164	AO	BL	1.0±0.1	2	1.2±0.15	0.83	≤ 0.05	2.28	-0.30	U
0256+075	OD094.7	Q	0.7±0.2	4	1.1±0.1	0.64	≤ 0.05			
0336-019		Q	1.3±0.1	3	2.0±0.2	0.65	≤ 0.05	2.82	-0.28	A
0400+258		Q	0.9±0.1	7	1.2±0.1	0.75	≤ 0.05	1.27	-0.13	U
0430+052	3C120	G	2.5±0.3	6	5.5±0.5	0.45	≤ 0.05	3.50	-0.12	A
0735+178		BL	1.6±0.4	10	2.4±0.2	0.67	≤ 0.05	2.20	-0.12	A
0736+017		Q	2.6±0.3	8	3.0±0.5	0.87	≤ 0.05	1.78	+0.14	?
0738+313		Q	0.6±0.1	5	1.6±0.15	0.38	0.1	1.62	-0.36	U
0742+103		EF	1.0±0.2	5	1.5±0.1	0.67	0.2	3.85	-0.49	U
0745+241		Q	0.4±0.1	6	1.3±0.15	0.31	0.3	1.08	-0.36	T
0748+126		Q	1.3±0.2	5	1.6±0.1	0.81	0.15	1.53	-0.06	A
0839+187		Q	0.8±0.15	5	0.8±0.15	1.0	≤ 0.05	1.02	-0.09	U
0851+202	OJ287	BL	1.1±0.3	12	1.3±0.15	0.85	0.1	2.33	-0.28	U
0906+015	4C+01.24	Q	0.8±0.15	9	1.4±0.2	0.57	0.1	1.52	-0.24	A
0953+254		Q	0.4±0.1	5	0.7±0.1	0.57	0.25	1.46	-0.47	?
1049+215	4C+21.28	Q	0.7±0.1	4	1.9±0.15	0.37	≤ 0.05	0.90	-0.09	T
1055+018	4C+01.28	Q	3.4±0.6	9	4.5±0.2	0.76	≤ 0.05	3.23	+0.02	A
1116+12	4C+12.39	Q	2.1±0.2	4	4.2±0.4	0.50	≤ 0.05	1.25	+0.19	A
1127-145		Q	4.6±1.2	5	5.0±0.2	0.92	≤ 0.05	4.52	+0.01	U
1145-071		Q	0.5±0.1	5	0.8±0.2	0.63	0.1	1.05	-0.27	?
1148-001	4C-00.47	Q	2.9±0.3	31	3.1±0.4	0.94	≤ 0.05	1.94	+0.15	A
1226+02	3C273	Q	16.2±2.0	14	72.0±6.0	0.23	≤ 0.05	30.50	-0.23	RA
1252+119		Q	0.9±0.2	5	0.9±0.1	1.0	0.1	0.84	+0.03	A
1253-055	3C279	Q	5.8±1.0	6	15.0±1.0	0.39	≤ 0.05	9.50	-0.18	T
1302-102		Q	0.3±0.1	6	0.8±0.2	0.38	0.15	0.78	-0.35	R?
1354-152		Q	0.6±0.1	6	0.8±0.1	0.75	≤ 0.05	2.42	-0.51	A
1504-166		Q	0.9±0.15	8	2.0±0.2	0.45	≤ 0.05	2.85	-0.42	?
1510-089		Q	1.5±0.25	6	3.5±0.3	0.45	0.15	3.30	-0.29	A
1514-241	AP Lib	BL	1.4±0.4	3	1.7±0.1	0.82	≤ 0.05	2.40	-0.20	U
1546+027		Q	0.5±0.1	3	1.0±0.1	0.50	0.1	2.27	-0.55	?
1550-269		EF	1.1±0.15	3	2.0±0.1	0.39	0.2			R?
1622-297		Q	1.6±0.15	6	2.7±0.2	0.59	0.15	2.45	-0.16	T
1741-038		Q	0.8±0.15	6	1.5±0.3	0.53	0.1	2.70	-0.45	U
2128-123		Q	1.3±0.1	3	1.6±0.1	0.81	0.15	3.10	-0.32	U
2131-021	4C-02.81	BL	1.7±0.3	5	1.9±0.2	0.89	≤ 0.05	2.67	-0.17	A
2145+067	4C+06.69	Q	2.8±0.5	4	3.8±0.5	0.74	≤ 0.05	2.53	+0.04	A
2155-152		BL	0.8±0.2	3	2.4±0.2	0.33	≤ 0.05	1.33	-0.19	T
2210-257		Q	0.9±0.15	4	1.5±0.2	0.60	0.1	1.23	-0.11	A
2223-05	3C446	Q	5.9±0.8	12	13.1±1.5	0.45	0.15			
2227-088		Q	1.1±0.15	4	1.1±0.1	1.0	≤ 0.05	1.13	-0.01	U
2243-123		Q	1.3±0.2	5	1.4±0.1	0.93	≤ 0.05	2.90	-0.29	A
2254+074	OY091	BL	0.5±0.15	8	0.7±0.2	0.71	0.3	0.37	+0.11	?
2318+049		Q	0.4±0.15	4	0.8±0.1	0.50	0.15	0.88	-0.29	A
2344+09	4C+09.74	Q	1.5±0.1	10	2.8±0.25	0.54	≤ 0.05	1.68	-0.04	
2354-117		Q	1.5±0.4	5	2.6±0.2	0.58	≤ 0.05			

3 Results

In Table 1, we present the results of the IPS observations at 327 MHz for the 57 sources. The columns are (1) the source name, (2) any other names, (3) optical identification, (4) flux density of the scintillating components, $S_c(327)$; the errors given are determined approximately by taking 1/2 to 1/4 of peak-to-peak variations of S_c depending upon the number of observations, (5) the number of days of IPS observations, (6) total flux density at 327 MHz, S_{327} , (7) the compactness parameter, i.e. the fraction of flux density in the scintillating components, $\mu_{327}=S_c/S_{327}$, (8) the angular size of the scintillating component, ψ , (9) the core flux density $S_c(5000)$ at 5 GHz taken from Perley (1982), (10) the spectral index of the core, α_{327}^{5000} (core), derived from values in columns 4 and 9, and (11) information about the radio structure with the symbols A, RA, R?, T, U, ? and NA indicating respectively that the source is asymmetric, resolved but asymmetric, resolved but structure not known, triple, unresolved, has uncertain structure, and no available data, at 5 GHz according to the VLA observations (Perley 1982; Ulvestad *et al.* 1981; VLA calibration list privately communicated).

Fig. 1 gives the histogram of μ_{327} for the 57 sources. It is found that the median value of $\mu_{327}=0.61\pm 0.05$. Of the 57 observed sources $\psi < 50$ and < 200 milliarcsec for 32 and 53 sources respectively. Thus about half of the flat-spectrum sources at 327 MHz have about 39 per cent of

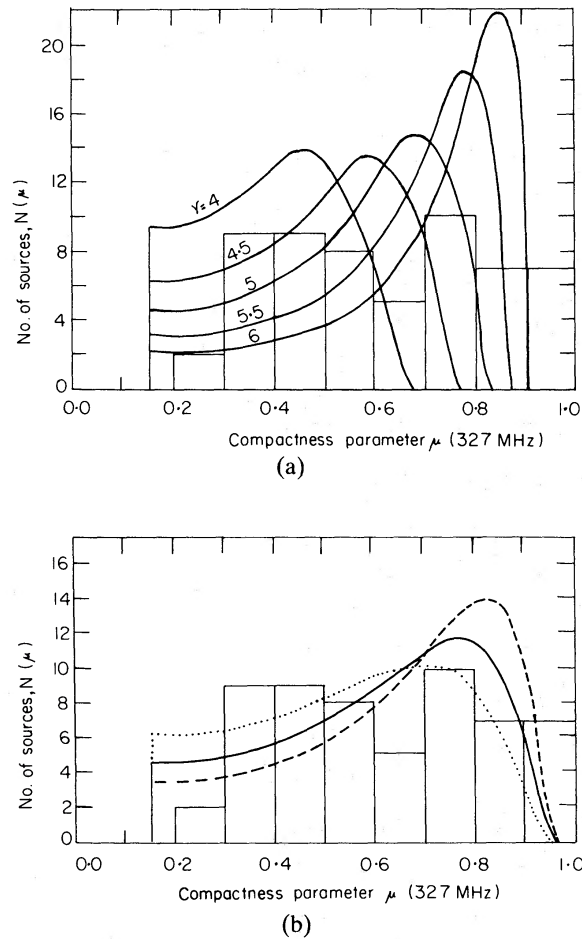


Figure 1. The observed distribution of the compactness parameter, μ_{327} , is shown by the histogram. In (a) the computed distributions for $\gamma=4, 4.5, 5, 5.5$ and 6 and $R_T=0.024$ are shown by full curves; (b) the computed curves for Gaussian distributions of γ are shown with mean values of 4.2 (dotted curve), 4.6 (full line) and 5.0 (broken line), $\Delta\gamma=2$ and $R_T=0.024$.

their flux density in non-scintillating large-scale structure with $\psi \geq 0.2$ arcsec and about 61 per cent in a compact core of size ≤ 0.05 arcsec. From Column 10 of Table 1, we find that, on average, the core of a flat-spectrum source has an inverted spectrum with an average spectral index α_{327}^{5000} (core) = -0.16 .

For 53 out of the 57 radio sources in Table 1, VLA observations have been made by Perley (1982) at 1.4 and 5 GHz with resolutions of about 1.2 and 0.4 arcsec respectively. He has given the flux densities of the cores (or upper limits) and also the peak brightnesses of the secondary structures. From these measurements we find that the median ratios of the peak brightnesses of secondary structures to those of the cores are about 3.5 and 0.5 per cent at 1.4 and 5 GHz respectively. Perley's data, however, do not give the flux densities contributed by any diffuse features. We have, therefore, estimated these values approximately from the VLA calibration list (private communication), which gives a summary of any variations in the interferometric visibilities. Such variations are caused by secondary compact and diffuse features related to the source and also by any unrelated sources in the field of view. The latter are more important at 1.4 GHz than at 5 GHz because of the wider field of view of the VLA at 1.4 GHz. By ignoring any contributions from the background sources, we estimate from the VLA visibility data that upper limits to the median ratios of the flux densities of the secondary compact and diffuse features to those of the cores are about 13 and 4 per cent at 1.4 and 5 GHz respectively.

Using MERLIN, which gives a resolution of about 0.5 arcsec at 966 MHz, Moore *et al.* (1981) have estimated that a flat-spectrum radio source has typically about 10 per cent of its flux density in extended features at 966 MHz. Thus it is seen that the fraction of flux density in extended components ($=1-\mu$) increases from about <0.04 at 5 GHz to ~ 0.1 at 966 MHz and 0.39 at 327 MHz.

From the VLA data for the 53 sources at 1.4 and 5 GHz, it is found that 15 sources are unresolved, with angular size $\psi \leq 0.2$ arcsec (See column 11 of Table 1), 20 have single secondary peaks, 6 have triple structure (classical double with a central component), 2 are resolved with asymmetric structure, 3 are resolved but no details are available about their structure and 7 have uncertain structure. It is interesting to note that $\mu_{327} > 0.7$ for 11 out of the 15 unresolved sources, as would be expected in the relativistic beaming model if the axes of these sources are aligned close to the line-of-sight and their core is not self-absorbed at 327 MHz. It may be noted further that, of 11 triple and resolved sources, $\mu_{327} < 0.4$ for 9 of them.

Perley (1982) has also given angular separations of the secondary peaks from the core. Not including the 10 sources with unknown structure, we estimate from the VLA data for the remaining 43 sources that the median value of the angular size is approximately 2.5 arcsec (for triple sources, we have considered only the distance to the outer component which is furthest from the core).

4 Discussion

In the scheme of OB82, flat-spectrum radio sources are simply those normal doubles whose axes point close to the line-of-sight. Using their model we have calculated the $N(\mu)$ distributions and compared these with our observations at 327 MHz and those by Moore *et al.* (1981) at 966 MHz.

4.1 THE $N(R)$ AND $N(\mu)$ DISTRIBUTIONS

On the assumption that the nuclear core emission of a double radio source arising from two oppositely directed relativistic jets is beamed whereas the extended features are not beamed, the observed ratio $R_v(\theta)$ of the flux density of the core to that of the unbeamed (extended)

components is given by (Scheuer & Readhead 1979; OB82)

$$R_\nu(\theta) = \frac{R_T}{2} [(1 - \beta \cos \theta)^{-2 + \alpha_c} + (1 + \beta \cos \theta)^{-2 + \alpha_c}], \quad (1)$$

where ν is the observing frequency, θ is the angle to the line-of-sight, β is the bulk velocity of the radio-emitting plasma in the jets corresponding to a Lorentz factor γ , $R_T = R_\nu(\theta=90^\circ)$, and α_c is the spectral index of the core. The minimum and maximum values of R_ν are R_T and $R_T \gamma^2 (2\gamma^2 - 1)$ for $\theta=90^\circ$ and 0° respectively, if $\alpha_c=0$. Because $\alpha_{400}^{5000} \leq 0.5$ for our sample of flat-spectrum sources, by taking the mean values of $\alpha_{327}^{5000} = -0.16$ and 0.9 as observed for the core and extended components respectively it can be shown that the lower limit to $R_{5000} = 3.3$ (see section 2.2 of OB82).

Since the sources are oriented randomly in sky, the probability distribution of R_ν is $P(R_\nu) dR_\nu = d(\cos \theta)$. It can be seen that the probability of occurrence of large R_ν , i.e. the pointing of the relativistic jet close to the line-of-sight, is small. On the other hand, the number counts of unbeamed steep-spectrum quasars increase with decreasing flux density as

$$N(>S_{\text{steep}}) \propto S_{\text{steep}}^{-\delta} \quad (2)$$

where $\delta \sim 1.5$ and $S_{\text{steep}} > S_0/(1+R_\nu)$, S_0 being the lower limit of the observed flux density of a sample of quasars with a specified value of R_ν . Hence, the distribution of R_ν is given by (OB82)

$$N(R_\nu) = \left(\frac{S_0}{1+R_\nu} \right)^{-\delta} \int_0^{z_{\text{max}}} \rho(z) P(R_\nu) dz, \quad (3)$$

where $\rho(z)$ is the redshift distribution of unbeamed quasars and is taken from fig. 11 of Wills & Lynds (1978) for their sample of quasars at 178 MHz.

Using (3) we first computed $N(R_{5000})$ taking $\delta=1.4$, $S_0=1$ Jy and the spectral indices of the core and extended components around 5000 MHz as 0 and 1 respectively for the sake of simplicity (OB82). Since $R = S_c/S_{\text{extended}}$, $N(R_{327})$ is readily derived from $N(R_{5000})$ by taking $\alpha_{327}^{5000} = -0.16$ for the core and $\alpha_{327}^{5000} = 0.9$ for the extended components. Finally, $N(\mu_{327})$ is determined by using the relation $\mu_{327} = R_{327}/(1+R_{327})$. It may be noted that $\mu_{327} > 0.15$, corresponding to $R_{5000} > 3.3$ as given above.

4.2 COMPARISON OF MODEL CALCULATIONS WITH OBSERVATIONS

The computed $N(\mu)$ distributions at 327 MHz for $R_T=0.024$ at 5000 MHz and $\gamma=4, 4.5, 5, 5.5$ and 6 are shown in Fig. 1(a), together with the observed $N(\mu)$ histogram at 327 MHz. It is seen that a single γ -value is not consistent with our observations. Hence, we smoothed the $N(R_{5000})$ distribution following OB82 and also considered a dispersion in R_T but these did not broaden the $N(\mu)$ curves sufficiently. In Fig. 1(b) are shown three computed curves for a Gaussian distribution of γ , with mean values of 4.2, 4.6 and 5.0, full half-width value $\Delta\gamma=2$ but $\gamma>1$, and R_T (5000 MHz)=0.024 as taken by OB82. The curve for $\gamma=4.6$ provides a satisfactory fit to the observed histogram. In Fig. 2 is shown a comparison of the results of this model with the observations at 966 MHz by Moore *et al.* (1981), where we have taken the observed data from their fig. 3 and converted their parameter r to μ_{966} by using the relation $\mu_{966} = 1/(r+1)$. The curve for $\gamma=4.6$ provides a satisfactory fit to the observed histogram. From the $N(\mu)$ distribution at various frequencies for $\gamma=4.6$, we find that the predicted median values of $(1-\mu)=0.36, 0.15$ and 0.03 at 327, 966 and 5000 MHz respectively, which are broadly consistent with the results given in Section 3. If we take $R_T=0.033$, as derived by Swarup, Sinha & Hilldrup (1984), the required value of $\gamma \sim 4.2$ and $\Delta\gamma=2$ for a satisfactory fit to our observations at 327 MHz.

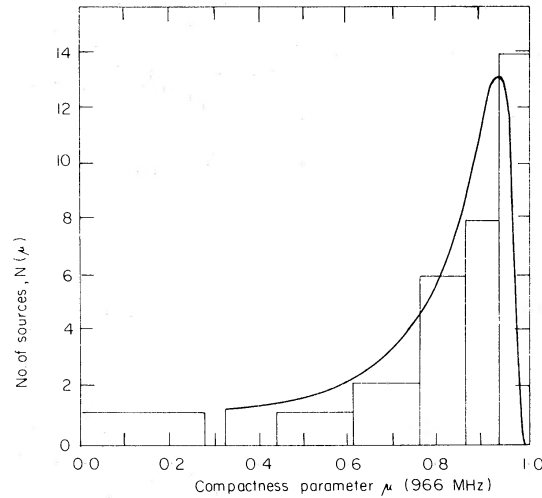


Figure 2. The observed distribution of the compactness parameter, μ_{966} , derived from the data of Moore *et al.* (1981) is shown by a histogram. The full line curve shows the computations for $\gamma=4.6$, $\Delta\gamma=2$ and $R_T=0.024$.

It has been shown by several authors (e.g. Perley *et al.* 1982; Browne *et al.* 1982) that the extended structure of flat-spectrum sources is more asymmetric than that of the classical doubles, with lobe brightness ratios being $>4:1$. This may arise either if the asymmetry is intrinsic, or if the sources are intrinsically symmetric but the emission of the mildly relativistic kiloparsec-scale jets or hotspots is Doppler boosted. The asymmetry could also arise from projection effects so that one of the radio lobes blends with the core but not the other, because of the typical misalignment by about 10 degrees of the two lobes of a double radio source; in this model there is a higher probability that the asymmetric component would be located further away from the observer and therefore its predictions are not quite consistent with the observations of a jet as well a hotspot in many of the asymmetric sources.

To explain the observed asymmetry, we have considered a three-component model (a combination of the models by OB82 and Moore *et al.* 1981) comprising a relativistic core ($\alpha=0$), mildly relativistic extended jets or hotspots ($\alpha=1$) and non-relativistic radio lobes ($\alpha=1$). Again the source axis is considered to lie close to the line-of-sight. To obtain the observed flux ratio of secondary components $\geq 4:1$, it is necessary to have values of $\beta \sim 0.4$ ($\gamma \sim 1.1$). Detailed calculations for the flux-density ratios of mildly relativistic hotspots have been made by Wilson & Scheuer (1983). The observed peak brightness values of the secondary structures of ~ 1 per cent at 5 GHz are explained by taking the fraction of flux density in hotspots as ~ 20 per cent. The values of γ , $\Delta\gamma$ and R_T are similar to those for the two-component model.

For a flat-spectrum source, the most likely value of the angle, ϕ , between the line-of-sight and the axis of the associated double source is about $1/\gamma\sqrt{5}$ (Moore *et al.* 1981). Taking $\gamma=4$, we obtain $\phi \sim 6^\circ$. Since the observed median value of the angular separation between the outer hotspots, LAS, is about 10 arcsec for a complete sample of 4C quasars (Wills & Lynds 1979), most of which are likely to be perpendicular to the line-of-sight, we expect that the typical angular separation between the secondary peaks and the central core of a flat-spectrum source is about $1/2 \text{ LAS} \sin \phi = 0.6$ arcsec. However, since the misalignment angle between the lines joining the outer hotspots and the central core is about 10° (Swarup *et al.* 1984), it can be shown that the median value of the observed angular separation of secondary peaks is predicted to be about $1/2 \text{ LAS} \sin 10^\circ \sim 1$ arcsec. These values are considerably smaller than the value of 2.5 arcsec estimated by us from the VLA data of Perley (1982) in Section 3, in which we have ignored 10 sources with uncertain structures.

It may be noted that, although the models considered here are not unique, the acceptable range of parameters is relatively narrow. The models can be improved only when more information becomes available regarding the asymmetric structures. This would require high-resolution observations (≤ 1 arcsec) for a complete sample of flat-spectrum sources at the longer wavelengths (≥ 30 cm), where the extended components become more prominent due to their steep spectrum.

Acknowledgments

The authors are grateful to Drs Gopal-Krishna and A. Pramesh Rao for valuable comments.

References

- Baars, J. W. M., Genzel, R., Pauliny-Toth, I. I. K. & Witzel, A., 1977. *Astron. Astrophys.*, **61**, 99.
- Brotten, N. W., Clarke, R. W., Legg, T. H., Locke, J. L., Galt, J. A., Yen, J. L. & Chisholm, R. M., 1969. *Mon. Not. R. astr. Soc.*, **146**, 313.
- Browne, I. W. A., Orr, M. J. L., Davies, R. J., Foley, A., Muxlow, T. W. B. & Thomasson, P., 1982. *Mon. Not. R. astr. Soc.*, **198**, 673.
- Galt, J. A., Brotten, N. W., Legg, T. H. & Yen, J. L., 1977. *Mon. Not. R. astr. Soc.*, **178**, 301.
- Kuhr, H., Witzel, A., Pauliny-Toth, I. I. K. & Nauber, U., 1981. *Astron. Astrophys. Suppl.*, **45**, 367.
- Large, M. I., Mills, B. Y., Little, A. G., Crawford, D. F. & Sutton, J. M., 1981. *Mon. Not. R. astr. Soc.*, **194**, 693.
- Moore, P. K., Browne, I. W. A., Daintree, E. J., Noble, R. G. & Walsh, D., 1981. *Mon. Not. R. astr. Soc.*, **197**, 325.
- Orr, M. J. L. & Browne, I. W. A., 1982. *Mon. Not. R. astr. Soc.*, **200**, 1067.
- Perley, R. A., 1982. *Astr. J.*, **87**, 859.
- Perley, R. A., Fomalont, E. B. & Johnston, K. J., 1980. *Astr. J.*, **85**, 649.
- Rao, A. P., Bhandari, S. M. & Ananthkrishnan, S., 1974. *Aust. J. Phys.*, **27**, 105.
- Scheuer, P. A. G. & Readhead, A. C. S., 1979. *Nature*, **277**, 182.
- Swarup, G., Sarma, N. V. G., Joshi, M. N., Kapahi, V. K., Bagri, D. S., Damle, S. H., Ananthkrishnan, S., Balasubramanian, V., Bhavne, S. S. & Sinha, R. P., 1971. *Nature Phys. Sci.*, **230**, 185.
- Swarup, G., Sinha, R. P. & Hilldrup, K., 1984. *Mon. Not. R. astr. Soc.*, **208**, 813.
- Ulvestad, J., Johnston, K., Perley, R. & Fomalont, E., 1981. *Astr. J.*, **86**, 1010.
- Wills, D. & Lynds, R., 1978. *Astrophys. J. Suppl.*, **36**, 317.
- Wills, D. & Lynds, R., 1979. *Astrophys. J. Suppl.*, **39**, 291.
- Wilson, M. J. & Scheuer, P. A. G., 1983. *Mon. Not. R. astr. Soc.*, **205**, 449.